Multiscale Symbolic Diversity Entropy: A Novel Measurement Approach for Time-Series Analysis and Its Application in Fault Diagnosis of Planetary Gearboxes

Yongbo Li, Shun Wang, Ni Li, and Zichen Deng

***Abstract*—The health condition monitoring of planetary gearboxes has drawn increasing attention due to the importance for safety operation and failure prevention. A novel diagnosis methodology based on multiscale symbolic diversity entropy (SDivEn) is proposed in this article. Herein, dynamical complexity of measured data is quantified by SDivEn. Compare to other entropy-based descriptors, SDivEn has advantages in its robustness and computation efficiency. To increase the feature representation capability of entropy descriptors, multiscale analysis is performed, where the measurement data in time series is decomposed into multiple scaled series by using the coarse graining process and then processed individually by using SDivEn method. The proposed multiscale SDivEn method is applied for fault recognition of planetary gearboxes. Experimental results indicate that the proposed method obtains the highest accuracy in recognizing seven health conditions of planetary gearboxes in comparison with three other existing entropy-based methods.**

***Index Terms*—Entropy, fault diagnosis, feature extraction, multiscale analysis, planetary gearboxes.**

I. Introduction

DUE to their large power transmission capacity and strong load-bearing capacity, the planetary gearboxes have been widely utilized in the large and complicated mechanical equipment, such as heavy trucks, aerospace, wind turbines, and other transmission systems. However, during operation, the key components of a planetary gearbox, including the ring gear, sun gear, and plane gear are particularly prone to damages due to heavy dynamic loading and highly rough and volatile operating environment. Any abnormal behaviors in planetary gearboxes are very likely to decrease the machinery's overall performance and cause severe economic losses in real applications. Therefore, health condition monitoring and fault diagnosis of planetary gearboxes play significant roles in preventing catastrophic failure and ensuring reliable operations of machineries [1].

In the past decades, much research has been done on dynamic modeling to study fault generation mechanism of gears [2], and further development of effective fault detection and diagnosis methods [3]. Moreover, the intelligent fault diagnosis based on feature extraction and pattern recognition methodology is a promising tool to accomplish the fault detection and fault diagnose [4]–[6]. Generally, the intelligent fault diagnosis method can be summarized into following three stages: data acquisition; feature extraction; and health condition pattern recognition. Among the three stages, the most critical stage is to extract representative features from the signals with strong background noises. In compare with many traditional feature extraction methods, entropy-based method has been demonstrated to be more effective [7].

As a powerful nonlinear signal analysis technique, entropy can quantify the regularity or orderliness for a given time series. When faults occur, the vibration response will change in its amplitude and frequency distributions, which can further influence the entropy. Therefore, the entropy-based methods can be utilized to detect the dynamic changes and further identify abnormal operations of planetary gearboxes. Compared with many other signal processing techniques, entropy-based methods are independent of manual experience and priori knowledge, and easy to implement. In recent years, several entropy-based methods have been developed and applied for the health condition monitoring and fault recognition, such as sample entropy (SE) [8], fuzzy entropy (FE) [9], and permutation entropy (PE) [10]. Zhang *et al*. [11] proposed a novel hybrid intelligent diagnosis method, which integrates PE, ensemble empirical mode decomposition, and optimized support vector machine (SVM). A fault diagnosis scheme is proposed by Cheng et al using entropy feature fusion and ensemble empirical mode decomposition [12]. Li *et al*. [13] proposed a new signal processing method by combining adaptive multiscale morphological filter and modified hierarchical PE for the diagnosis of planetary gearboxes. Meanwhile, a novel signal processing methodology

Manuscript received April 9, 2021; accepted May 17, 2021. Date of publication May 24, 2021; date of current version October 27, 2021. This work was supported by the National Natural Science Foundation of China under Grant 51805434. Paper no. TII-21-1602. *(Corresponding author: Yongbo Li.)*

The authors are with the School of Aeronautics, Northwestern Polytechnical University, Xi'an 710072, China (e-mail: yongbo@nwpu.edu.cn; wangshun@mail.nwpu.edu.cn; lini@nwpu.edu.cn; dweifan@nwpu.edu.cn).

Color versions of one or more figures in this article are available at https://doi.org/10.1109/TII.2021.3082517.

Digital Object Identifier 10.1109/TII.2021.3082517

based on Vold–Kalman filter and multiscale SE was proposed to accomplish diagnosis of planetary gearboxes. Unfortunately, these existing entropy methods do not work well under strong background noises without assistance of a denoising process. In addition, these existing entropy methods have disadvantages in the analysis of short time series and have low calculation efficiency [14].

In this article, to solve the above deficiencies, a new entropy algorithm called symbolic diversity entropy (SDivEn), based on symbolic dynamic filtering (SDF) and distribution probability is proposed. SDivEn is composed of the following three steps: first, an SDF procedure is utilized to reduce measurement noise and convert the measurement in time series to symbolic sequences, Second, these symbolic sequences are further used to reconstruct the phase information between states. Third, the cosine similarity between successive states is calculated to represent the probability distribution of the state patterns. Due to its noise reduction capability and data compression capability, SDivEn method is robust and timesaving in performance. Multiple simulated signals are applied to prove the more significant performance of SDivEn in consistency, robustness to noises, and calculation efficiency compared with SE, FE, and PE. Moreover, to increase the feature representation capability of entropy descriptors, multiscale analysis is performed, where the measurement data in time series is decomposed into multiple scaled series by using the coarse graining process and then processed individually by using SDivEn method. The proposed multiscale SDivEn (MSDivEn) is applied in the condition recognition of planetary gearboxes, and compared with multiscale SE (MSE) [15], multiscale FE (MFE) [16], and multiscale PE (MPE) [11]. The comparison diagnosis results indicate that the proposed MSDivEn performs best in fault recognizing of planetary gearboxes and gets the highest classification accuracy.

Overall, the proposed MSDivEn method provides an attractive avenue for the entropy-based method in noise cancelling and calculation efficiency enhancement. First, SDivEn is first developed to extract the fault information with strong background noises. Then, SDivEn is further extended into multiscale analysis, namely MSDivEn, for rich fault symptom description. Finally, we demonstrate that our proposed MSDivEn method performs best in tracking changes of dynamical behavior and recognizing different health conditions of planetary gearboxes via both simulated and experimental data.

The rest of this article is organized as follows. Section II first introduces the basic concepts and the procedure of proposed method. In Section III, simulations are carried out to validate the advantages of the proposed method. In Section IV, the effectiveness of the proposed method in fault condition recognition is demonstrated by one case study. Finally, Section V concludes this article.

II. Methodology

A. Symbolic Diversity Entropy

SDivEn employs a three-step procedure to improve the computation efficiency and robustness of existing entropy methods. First, an SDF procedure is utilized to reduce measurement noise and convert the measurement in time series to symbolic sequences. Second, these symbolic sequences are further used to reconstruct the phase information between states. Then, the cosine similarity of adjacent states is utilized to measure similarity and the concept of distribution is introduced, where the probability distribution of pattern similarity is utilized to describe the pattern changes.

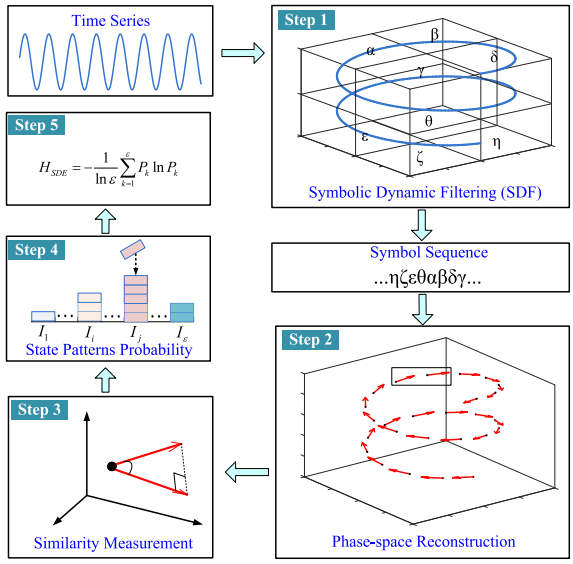

Fig. 1. Schematic diagram of SDivEn. (In step 1, "$\eta\zeta\varepsilon\theta\alpha\beta\delta\gamma$" represents the symbolic sequence after SDF; In step 4, "$I_1, I_2, \ldots, I_\varepsilon$" represents the partitioned ε intervals for cosine similarity, and $P_1, \ldots, P_\varepsilon$ is corresponding state probability).

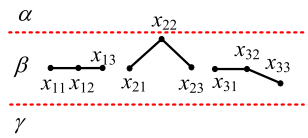

Fig. 2. Schematic diagram of resisting the noise and fluctuations.

For a time series $S = \{s_1, \ldots, s_i, \ldots, s_N\}$ with length N, the detailed procedure of SDivEn can be calculated following five steps and the schematic diagram is illustrated in Fig. 1.

Step 1: Encode the raw time-series Sinto the symbol time series of ε symbols $y = \{y_1 y_2 \cdots y_N\}$. As shown in Fig. 1, the continuous state space is converted into the discrete state space through SDF, so that the symbol sequence can be obtained. In this article, maximum entropy partitioning (MEP) is applied to symbolize the raw time series. Because variations in data patterns are more likely to be reflected in the symbol sequence, which are obtained using MEP than other partition approaches [17].

According to researches [17]–[20], the procedure of SDF is robust to measurement noise and spurious disturbances. Partitioning the continuous data into finite blocks and generation of a symbol sequence can reduce measurement noise. An example is provided to illustrate the noise with small fluctuations can be effectively removed. As shown in Fig. 2, $X_1 = \{x_{11}, x_{12}, x_{13}\}$ represents the initial sequence, $X_2 = \{x_{21}, x_{22}, x_{23}\}$and $X_3 =$

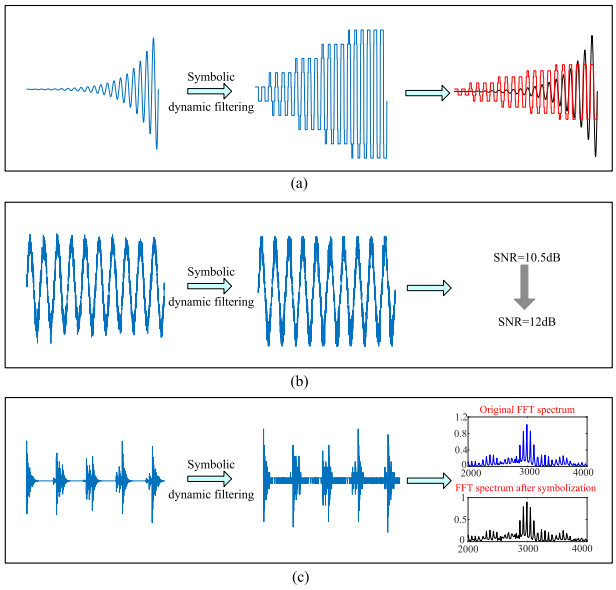

Fig. 3. Advantages of SDF. (a) Reservation of amplitude characteristics. (b) Enhancement of SNRs. (c) Reservation of frequency distribution characteristics.

$\{x_{31}, x_{32}, x_{33}\}$ represent the sequence after noise interference. As a result of noise interference, the amplitude of the time series will fluctuate around the true value. Through SDF procedure, the sequences become the same, as $\{\beta, \beta, \beta\}$. Thus, SDF has advantage of resisting the noise and fluctuations.

For a better understanding of the advantages of SDF, Fig. 3 gives a clear illustration. As shown in Fig. 3(a), it can be observed that it works well in tracking the dynamic change of signals using encoding strategy. Seen from Fig. 3(b), it can be seen that the symbolization can directly enhance the signal-to-noise ratios (SNRs) [21]. Through SDF procedure, the SNR of time series are increased to 12 from 10.5 dB. In Fig. 3(c), the time series is converted into a symbolic sequence and fast Fourier transform (FFT) analysis is conducted. From Fig. 3(c), it can be observed that the sideband of intrinsic frequency is not discarded and the frequency distribution is well reserved. This phenomenon indicates that the fault information can be reserved effectively after symbolization process. Therefore, the symbolization of time series has the merits in information reservation and SNR enhancement.

Step 2: Based on Taken's Embedding theorem, construct the state vector $X_i^m = \{y_i, y_{i+\lambda}, \ldots, y_{i+(m-1)\lambda}\}$ in a phase space with a dimension of m and time lagged variable of λ as follows:

$$X(m) = \left[X_1^m, \ldots, X_i^m, \ldots, X_{N-(m-1)\lambda}^m\right]^T = \begin{bmatrix} y_1 & y_{1+\lambda} & \cdots & y_{1+(m-1)\lambda} \\ \vdots & \vdots & \vdots & \vdots \\ y_i & y_{i+\lambda} & \cdots & y_{i+(m-1)\lambda} \\ \vdots & \vdots & \ddots & \vdots \\ y_{N-(m-1)\lambda} & y_{N-(m-1)\lambda+\lambda} & \cdots & y_N \end{bmatrix}. \quad (1)$$

As illustrated in the step 2 of Fig. 1, through phase-space reconstruction, a series of vectors can be obtained.

Step 3: Measure the similarity between the adjacent symbol sequences using cosine similarity. Then, a series of cosine similarities$(\mathrm{Sim}_1, \ldots \mathrm{Sim}_i, \ldots, \mathrm{Sim}_{N-(m-1)\lambda-1})$ can be obtained. The cosine similarity between two symbol sequences X_i^m andX_{i+1}^m is expressed as

$$\begin{aligned} \mathrm{Sim}_i &= \mathrm{Sim}(X_i^m, X_{i+1}^m) \\ &= \cos(X_i^m, X_{i+1}^m) \\ &= \frac{X_i^m \cdot X_{i+1}^m}{\|X_i^m\| \left\|X_{i+1}^m\right\|}. \end{aligned} \quad (2)$$

As shown in the step 3 of Fig. 1, cosine similarity measures the similarity between two symbol sequences of an inner product space by the cosine of the angle between two vectors. Note that since symbol sequence is positive after symbolization, the range of the cosine similarity Sim_i is [0, 1]. Obviously, a large cosine similarity represents that there are dynamical changes of similarity, predictability, or periodicity between two sequences. On contrary, a small cosine similarity indicates a dynamical phenomenon of diversity, stochasticity, or chaos.

Step 4: Partition the range [0, 1] of cosine similarity into ε intervals denoted by $I_1, I_2, \ldots, I_\varepsilon$, as shown in the step 4 of Fig. 1. Next, we count the quantity of falling into each interval I and obtain the state probability $(P_1, \ldots, P_\varepsilon)$.

Step 5: Define the SDivEn value by the classical formula of Shannon entropy, which can be expressed as

$$\mathrm{SDivEn}(m, \lambda, \varepsilon) = -\frac{1}{\ln \varepsilon} \sum_{k=1}^{\varepsilon} P_k \ln P_k. \quad (3)$$

The pseudocode of SDivEn can be seen in algorithm 1. Here, the entropy is the measure of signal complexity. The larger the entropy, the more complex the signal. Thus, the value of SDivEn is monotone and increases in the range of [0, 1] as the increasing of complexity. Physically speaking, SDivEn tending to 0 indicates that the time series is with a low complexity, such as a constant signal, sine signal, or periodic signal. In contrast, a larger SDivEn value indicates that the time series is more stochastic and irregular, which contains high complexity.

B. Multiscale Symbolic Diversity Entropy

However, SDivEn is a single-scale analysis approach, which describes the characteristics at only one scale and contains poor feature information. To increase the feature representation capability of entropy, multiscale analysis is performed. Multiscale analysis is proposed by Costa, which can represent the complexity of a time series over a range of scales. Therefore, multiscale SDivEn (MSDivEn) is further proposed to describe the fault characteristics over multiple scales. In this method, the measurement data in time series is decomposed into multiple scaled series by using the coarse graining process and then processed individually by using SDivEn. The detailed procedure is given as follows.

Algorithm 1: Symbolic Diversity Entropy.

Input: Time series $S = \{s_1, \ldots, s_i, \ldots, s_N\}$, embedding dimension m, and the number of symbols ε, time lagged variable λ.

Output: SDivEn

Encode the time series S into symbol time series $y = \{y_1 y_2 \cdots y_N\}$with ε symbols.
$M = N - (m-1)\lambda$
for $i = 1$:M do
  for $j = 1$:m do
    $X(i,j) = y(i + (j-1)\lambda)$
  end for
end for
for $i = 1$: M-1 do
  $\mathrm{Sim}_i = \mathrm{Sim}(X_i^m, X_{i+1}^m) = \cos(X_i^m, X_{i+1}^m)$
end for
  $[A] = \mathrm{histcounts}(\mathrm{dist}, 0 : \frac{1}{\varepsilon} : 1)$
  $P = A/\mathrm{sum}(A)$
  $\mathrm{SDivEn} = -\frac{1}{\ln \varepsilon} \sum_{k=1}^{\varepsilon} P_k \ln P_k$

Step 1: Given a time series $X = \{x_1, x_2, \cdots, x_n\}$, divide it into coarse-grained series $y^{(k)} = \{y_1^{(k)} \ldots y_p^{(k)}\}$, $p = [\frac{N}{k}]$, $1 \le k \le \tau$ according to

$$y_j^{(k)} = \frac{1}{k} \sum_{i=(j-1)k+1}^{jk} x_i, 1 \le j \le \frac{N}{k} \tag{4}$$

where $1 \le k \le \tau$. To obtain the coarse-grained time series at the scale factor of k, the original time series is divided into non-overlapping windows of length k and the data points inside each window are averaged. The original time series has a scale factor of $\tau = 1$, and it can be represented by $y^{(1)}$.

Step 2: Compute *SDivEn* value to quantify the stochasticity or irregularity of the coarse-grained time series, which can be expressed as:

$$\mathrm{MSDivEn}(X, \tau, m, \varepsilon, \lambda) = \mathrm{SDivEn}(y^k, m, \varepsilon, \lambda), 1 \le k \le \tau. \tag{5}$$

The pseudocode of MSDivEn can be seen in algorithm 2.

Algorithm 2: Multiscale Symbolic Diversity Entropy.

Input: Time series$X\{x(n), n = 1, 2, \ldots, N\}$, embedding dimension m, the number of symbols ε, time lagged variable λ, and the scale factor τ.

Output: Multiscale symbolic diversity entropy (MSDivEn)

for k = 12, …,τ do
  obtain the coarse-grained time series $y^{(k)} = \{y_1^{(k)} y_2^{(k)} \ldots y_p^{(k)}\}, p = [\frac{N}{k}]$
  Compute the SDivEn valve of $y^{(k)}$
Augment the data $\mathrm{MSDivEn}_{1:k} = \{\mathrm{MSDivEn}_{1:k-1}; \mathrm{SDivEn}(y^k, m, \varepsilon, \lambda)\}$
end for.

C. Fault Diagnosis of Planetary Gearboxes

The proposed fault diagnosis method using MSDivEn consists of two stages. First, extract the fault information from vibration signals of planetary gearboxes using MSDivEn. Next, SVM is applied as a classifier to identify different health conditions since SVM has a high computing efficiency, which is simple and easy to be implemented. This two-stage method can be further broken into the following four steps.

1) Collect the vibration signals of planetary gearboxes under various conditions.
2) Extract fault features using MSDivEn.
3) Train SVM classifier using the obtained fault features.
4) Test the trained classifier and obtain the diagnosis results.

III. Simulation Evaluation

The proposed SDivEn method has the following three advantages: high consistent performance regardless of data length; robustness to the noise; and high calculation efficiency. To demonstrate these advantages, SDivEn is compared with other three used commonly entropy methods, including SE, FE, and PE by using some simulated signals. The corresponding parameters are selected following the in [11] and [16]. SDivEn: dimension $m = 3$, time lagged variable $\lambda = 2$, the number of symbols ε= 20, SE: dimension m = 2, the tolerance for accepting matches $r = 0.15$, PE: dimension $m = 5$, and FE: dimension m = 2, the tolerance for accepting matches $r = 0.15$.

A. Consistency

Consistency measures the influence of data length and its complexity estimation value. Here, the white Gaussian noise (WGN) and 1/*f* noise with different data points are utilized to test the performance of four methods in consistency. The length of two noises varies from 50 to 1000 with interval 50. To reduce the effects of the randomness, 100 trials are carried out using four methods: SDivEn; SE; FE; and PE, and the average values with its corresponding error bars are calculated.

From the analysis results using 1/*f* noise and WGN as shown in Fig. 4(a) and (b), respectively, it can be found that SE and FE generate large error bars when analysis of short time series, especially for data points $N < 600$. Moreover, the undefined SE values may occur when the data points $N < 100$. This phenomenon indicates SE and FE methods have restrict requirements for the data length. As suggested in[22], the length of the time series is suggested to be in the range of 10 to 30 m to obtain a reasonable SE and FE value, so that it will limits its applications in analysis the short time series especially combination with the multiscale analysis.

On the contrary, PE and our proposed SDivEn methods can both generate smaller error bars, and thus be almost free of data length influence. However, it can be observed that PE values show an increasing trend with poor consistency for data points $N < 200$, while our proposed SDivEn method approximates to

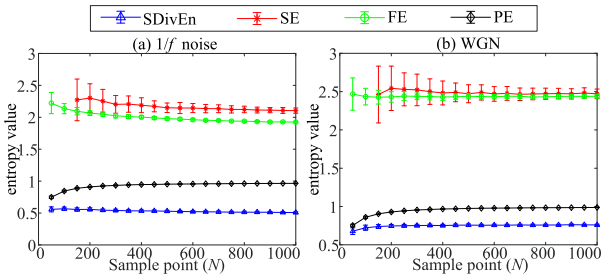

Fig. 4. Analysis results of 100 independent 1/*f* noise and WGN with different data points using SDivEn, SE, FE, and PE method. (a) Analysis results of 1/*f* noise. (b) Analysis results of WGN.

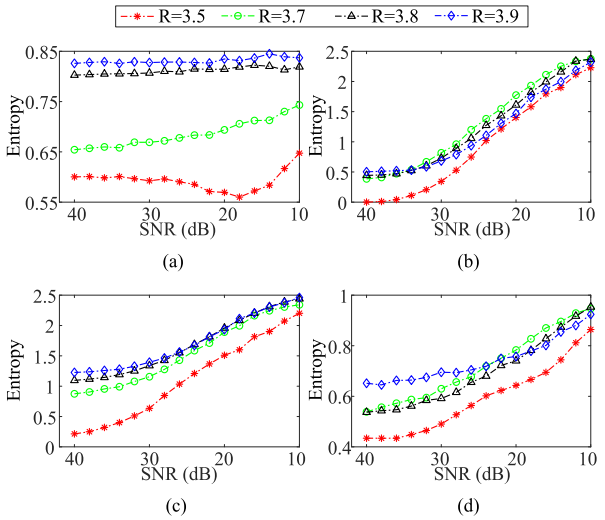

Fig. 5. Performances of the four entropy statistics on distinguishing Logistic systems at different SNR values. (a) Symbolic diversity entropy. (b) Sample entropy. (c) Fuzzy entropy. (d) Permutation entropy.

a constant line as shown in Fig. 4. This phenomenon indicates that SDivEn is less depended on the time series length so that it is valid in analyzing short time series and SDivEn has strong relative consistency of different data points.

B. Robustness

To investigate the noise robustness of SDivEn, logistic datasets $\{x|x_{i+1} = Rx_i(1 - x_i)\}$ (where x_1 is set as 0.1) for R = 3.5, 3.7, 3.8, and 3.9 are applied. The time series are generated after a transient period of 1000 points with data length $N = 2000$. It should be noticed that $R = 3.5$ generates the periodic (period four) dynamics with $R = 3.7$–3.9 produce chaotic dynamics with increasing complexity. Here, the entropy, which is the measure of stochasticity, should exhibit higher entropy values for chaotic dynamics than periodic dynamics. Therefore, the entropy values of four signals, theoretically, are listed as: $\mathrm{En}_{R=3.5} < \mathrm{En}_{R=3.7} < \mathrm{En}_{R=3.8} < \mathrm{En}_{R=3.9}$. Also, after adding the noise, the same order of complexity should be kept. The noises with different SNR are added into logistic datasets to test the robustness. Note that the SNR of four signals varies from 40 to 10 dB with interval

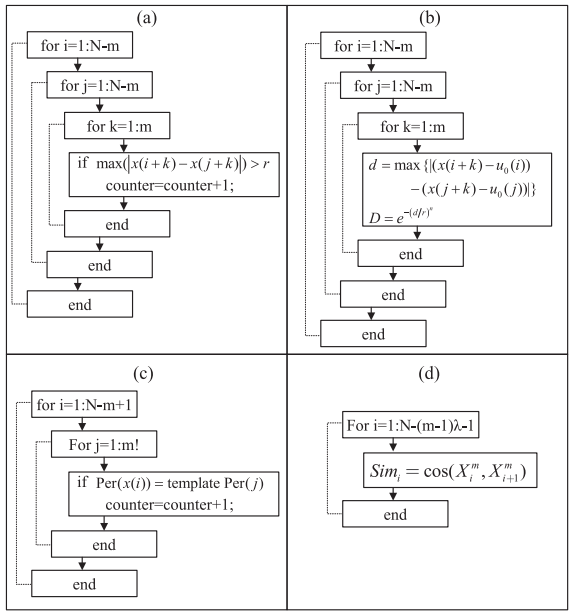

Fig. 6. Main calculation loop of four entropy methods. (a) Sample entropy. (b) Fuzzy entropy. (c) Permutation entropy (per indicates permutation). (d) Symbolic diversity entropy.

of 2 dB. Fig. 5 shows the performance results on distinguishing Logistic systems with different SNR values.

From Fig. 5, when SNR = 40, only the PE curves are not consistent with the complexity arrangement of different R values. By contrast, SE, FE, and SDivEn all can correctly distinguish the datasets of different parameter R. However, as noise is superimposed and SNR decreases, the distinction between the logistic systems turns out to be different. In Fig. 5(b), when the noise level comes up to 36 dB, there is mixing phenomena for SE method. Similarly, from Fig. 5(c), when the SNR decreases to 26 dB, FE fails in the system distinction. In Fig. 5(d), PE cannot distinguish the logistic datasets of different R correctly from 40 to 10 dB. Among four methods, only the SDivEn statistics can correctly distinguish the datasets over different noise levels, as shown in Fig. 5(a). This comparison results visually verify that the proposed SDivEn is the most robust than other entropy methods, and it offers a more practical approach that will work under conditions with high background noise.

C. Calculation Efficiency

To investigate the calculation efficiency of SDivEn, the time complexity is calculated. For comparison, the time complexity of SE, FE, and PE are also listed as $O(N^2)$, $O(N^2)$, and $O(N)$, respectively, as shown in Fig. 6. We assume that all elementary operations take the same value of time. SDivEn has a temporal complexity of $O(N)$ according to the definition of SDivEn in Algorithm 1, as shown in Fig. 6(d).

To compare intuitively the calculation efficiency, the running time of Section III-B is counted. The computer configuration is Core I7-6700HQ @2.6GHz and 16GB RAM with MATLAB R2018a and the results for each method are given in Table I. The obtained results visually show that our proposed SDivEn

TABLE I
TIME COMPLEXITY AND CALCULATION TIME OF FOUR ENTROPY METHODS

Method	SE	FE	PE	SDivEn
Time complexity	O(N^2)	O(N^2)	O(N)	O(N)
Calculation time (s)	39.59	95.80	3.19	0.59

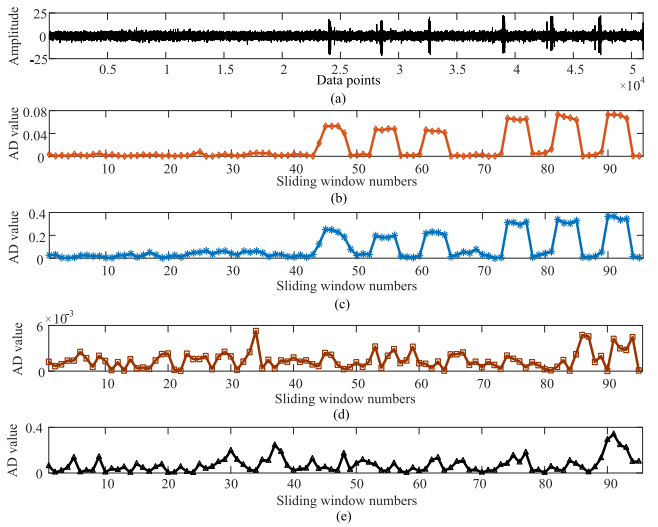

Fig. 7. Performances of four entropy statistics on impulse detection. (a) Waveform of the synthetic gearbox signal. (b) Symbolic diversity entropy. (c) Fuzzy entropy. (d) Permutation entropy. (e) Sample entropy.

consumes the least amount of time. It further confirms that SDivEn has a desirable calculation efficiency and it can be used in online condition monitoring of machinery.

D. Impulse Detection

To confirm the effectiveness of SDivEn in detecting gear fault severities, the synthetic planetary gear faulty signals have been constructed according to [23]. Here, the planetary gearbox with normal condition and different cracked fault severities are considered in the simulated study. In addition, the white Gaussian noise SNR $= -5$ dB is added to simulate the noisy environment. The time-domain waveform of the simulated signal is illustrated in Fig. 7(a). A comprehensive comparison analysis is conducted between the SE, FE, PE, and SDivEn methods. Note that the length of simulated signal is 51 000 and the signal is cut out using the sliding windows of 2048 with a moving step length of 512, which means a sliding window data with 25% overlap moving along the signal.

Here, the absolute difference value between the average entropy value of the first 10 samples (normal samples) and entropy value of other samples is computed to assess the impulse detection ability. The obtained results are illustrated in Fig. 7 (b)–(e). Seen from Fig. 7(b)–(e), it can be observed that only SDivEn and FE are able to detect the impulses. However, the proposed SDivEn shows better robustness for noise than FE method, which can even clearly differentiate two fault severities. The fault detection performance of four methods is listed as: SDivEn>FE>PE>SE. The comparison results indicate that the proposed SDivEn method can greatly enhance the impulse detecting ability.

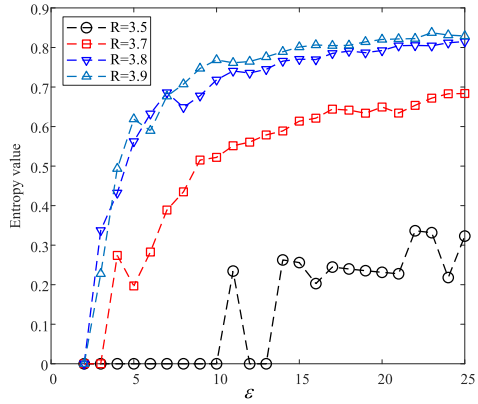

Fig. 8. Performance of SDivEn with different parameter ε.

E. Parameter Selection Analysis

There are four parameters needed to be set before using MSDivEn method including $m, \varepsilon, \lambda \text{and} \tau$. Just like PE and SE, the time delay λ has little influence on the results [24], we recommend to set λ=2. The dimension m of SDivEn represents the length of sequences to be compared. A larger m allows more detailed reconstruction of the dynamic process. Conversely, if the dimension m is too large, it requires long time series, which cannot be realized in real-case application [25]. Following[26], m is fixed to 3 in this article. The scale factor τ relates to the dimension of features. Because a smaller scale number will eliminate the performance in feature extraction, while a larger scale will result in dimension disaster and enhance the CPU time [9]. Therefore, here, we recommend to set τ=10to20 in this article.

The parameter ε is the number of symbols. To evaluate the performance of SDivEn with different parameterε, the Logistic datasets $\{x|x_{i+1} = Rx_i(1 - x_i)\}$ (where x_1 is set as 0.1) for R = 3.5, 3.7, 3.8, and 3.9 are applied for parameter ε selection. The time series are generated after a transient period of 200 points and the data length is $N = 1000$. Theoretically, the entropy values of four signals are listed as: En $_{R\ =\ 3.5}<$ En $_{R\ =\ 3.7}<$ En $_{R\ =\ 3.8}<$ En $_{R\ =\ 3.9}$. The obtained entropy values with different ε values are shown in Fig. 8. When $\varepsilon = 2\text{to}7$, the entropy curves are not consistent with the complexity arrangement of different R values. Moreover, there is mixing phenomena when $\varepsilon = 3\text{and}6$. When $\varepsilon = 8$, the SDivEn value with different R values are in good agreement with the actual ones. In general, as more symbols are incorporated, the antinoise ability can be reduced. While, less symbols will result in SDivEn cannot extract enough fault information. Hence, ε is suggested to set 10–20, and we select $\varepsilon = 20$ in this article.

IV. EXPERIMENT EVALUATION

An experiment is carried out to evaluate the performance of proposed method for health diagnosis of a planetary gearbox.

A. Test Rig

The experiment is conducted on an industrial planetary gearbox system located at Shandong University, as shown in Fig. 9(a) [27]. The planetary gearbox is composed of the driving motor,

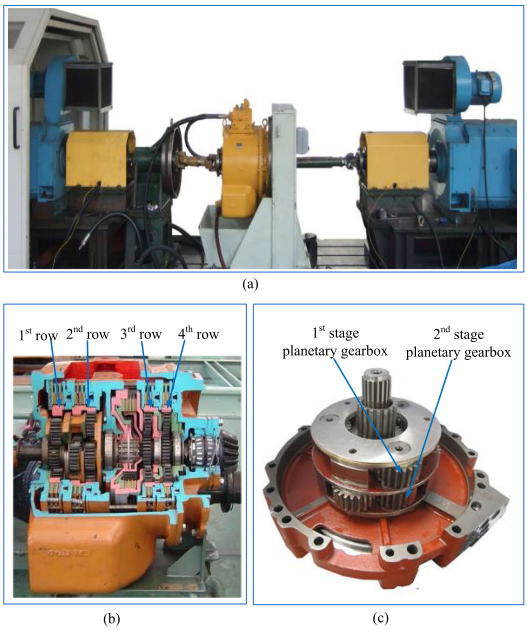

Fig. 9. Planetary gearbox experiment system. (a) Experimental test rig. (b) Planetary gearboxes. (c) Second row of planetary gearbox [27].

TABLE II
PARAMETERS OF THE EXPERIMENTAL TEST RIG

Gearbox	First gear stage			Second gear stage			Carrier
Gear	Sun	Planet	Ring	Sun	Meshed-planet	Ring	
No. of teeth	30	21	72	30	21	78	
rotational speed(HZ)	0	816	476	700	184	856	476	336

control unit, load device, cooling system, one fixed-speedup gearbox, and one test-planetary gearbox. Fig. 9(b) and (c) presents the industrial test-planetary gearbox. The industrial test-planetary gearbox can accomplish three forward and backward gear rotations via the five gear stages and clutches. We design the experiment on the first planetary gear and second meshed-planet gear, which are connected via carrier. To measure the vibration signals, one three-axis vibration acceleration sensor is mounted on the gearbox casing. The parameters of these compound gears set is given in Table II. Note that the transmission ratio is 2.08. In the case study, eight condition types of compound planetary gear are considered. The damage types consist of the broken tooth, cracked tooth and pitting tooth occurring on both sun gear and planet gear of first and second stages. Fig. 10 presents the photos of damaged gears, including broken tooth on planet gear, broken tooth on ring gear, broken tooth on sun gear, cracked tooth on sun gear, and pitted tooth on sun gear. Here, the sampling frequency of data acquisition system is set to be 5120 Hz. The 200 N·m load is designed to simulate the real application scenario with rotation speed of 700 PRM.

For each working condition, the collected data are divided into several overlapping samples. It is noticed that each health condition has 100 samples. Each sample contains 2048 data

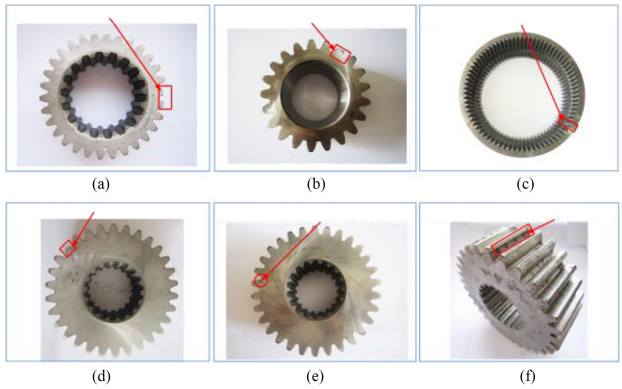

Fig. 10. (a) Broken tooth on sun gear of first stage (BTSG). (b) Broken tooth on planet gear of second stage (BTPG). (c) Broken tooth on ring gear of second stage (BTRG). (d) Broken tooth on sun gear of second stage (BTSG). (e) Cracked tooth on sun gear of second stage (CTSG). (f) Pitted tooth on sun gear of second stage (PTSG).

TABLE III
DETAILED ARRANGEMENTS OF THE EXPERIMENTAL DATA

Health conditions		Class label	Number of training data	Number of testing data
First stage	Second stage			
Normal	Normal	1	75	25
BTSG	Normal	2	75	25
BTPG	Normal	3	75	25
Normal	BTPG	4	75	25
Normal	BTRG	5	75	25
Normal	BTSG	6	75	25
Normal	CTSG	7	75	25
Normal	PTSG	8	75	25

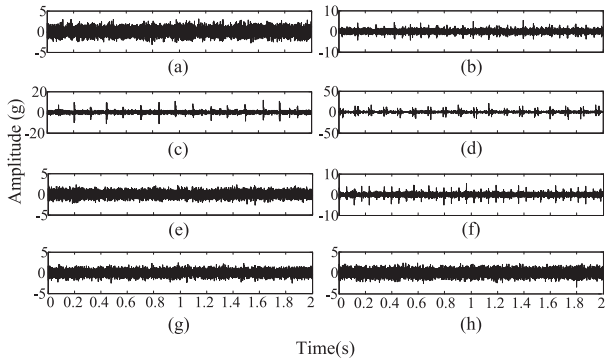

Fig. 11. The vibration signals of each health condition for planetary gearbox. (a) Normal. (b) BTSG of first stage. (c) BTPG of first stage. (d) BTPG of second stage. (e) BTRG of second stage. (f) BTSG of second stage. (g) CTSG of second stage. (h) PTSG of second stage.

points and there are total 800 samples. These details are given in Table III. Also, Figs. 11 and 12 illustrate the corresponding time-domain waveforms and FFT spectra with eight health conditions, respectively.

B. Experimental Results

For comparison purposes, MSE, MFE, and MPE are all applied to extract fault features, and the obtained features are

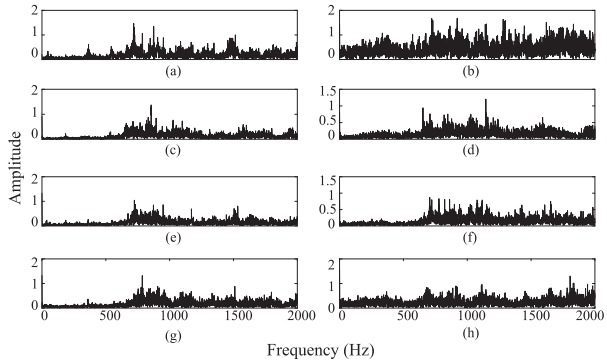

Fig. 12. Spectra of eight health conditions. (a) Normal. (b) BTSG of first stage. (c) BTPG of first stage. (d) BTPG of second stage. (e) BTRG of second stage. (f) BTSG of second stage. (g) CTSG of second stage. (h) PTSG of second stage.

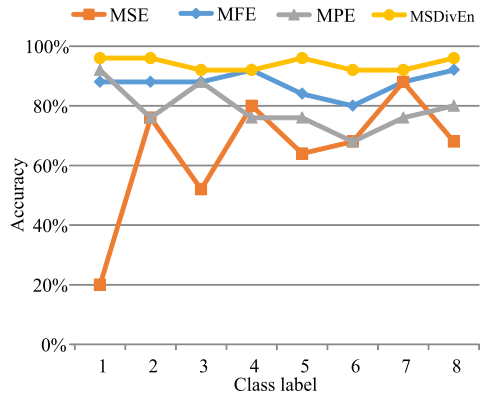

Fig. 13. Classification accuracies of four methods under eight working conditions.

used as input in the SVMs for pattern identification. The parameter optimization of the SVM classifier is obtained by using a grid-search technique with five-fold cross-validation so that the optimal penalty parameter C and the kernel parameter γ of radial-basis function kernel can be determined [28]. Note that the scale factor $\tau = 15$ in the experiment and we can obtain 15 features. The diagnosis results are shown in Fig. 13.

It can be seen from Fig. 13 that the classification accuracy of the MSDivEn-SVM has the highest classification accuracy compared with MSE-SVM, MFE-SVM, and MPE-SVM in all working conditions. The diagnostic performance of these four methods follows a decreasing order of MSDivEn > MFE > MPE > MSE. The comparison results can be explained in the following way. Compared with other entropy methods, MSDivEn method has the advantage of resisting noises by using SDF while maintaining the fault information of vibrations. Hence, the fault information embedded in vibration signal can be extracted from strong the background noises. Moreover, the utilization of cosine similarity and distribution can describe the state distribution using the statistical probability of pattern similarity with high accuracy. This will enhance the generalization ability and fault diagnosis performance of MSDivEn-SVM with low standard deviation value. Meanwhile, the accuracy of MFE is higher than MSE because MFE has used the fuzzy set theory, which enhances the performance in dynamic detection with a more accurate complexity estimation results.

TABLE IV
CLASSIFICATION RESULTS OF PLANETARY GEARBOX

Method	Mean testing accuracy	Standard deviation	Average time(s)
SDivEn-SVM	55.42%	2.71%	6.84
SE-SVM	52.47%	2.68%	264.09
FE-SVM	69.80%	2.69%	1023
PE-SVM	39.93%	2.35%	33.5
MSDivEn-SVM	**93.42%**	**1.30%**	**20.01**
MSE-SVM	64.45%	3.63%	431.95
MFE-SVM	87.83%	2.02%	1616
MPE-SVM	76.10%	2.68%	110.06

To reduce the randomness effect, 20 trials are conducted for each method, and then the average accuracy and elapsed time of feature extraction is computed for each method. The results are illustrated in Table IV. Seen from Table IV, it can be found that MSDivEn-SVM, MPE-SVM, MFE-SVM, and MSE-SVM obtain higher recognition accuracy than SDivEn-SVM, PE-SVM, FE-SVM, and SE-SVM. The phenomenon indicates that multiscale analysis can extract more feature information over different scales, which can prove the effectiveness of the multiscale analysis. Moreover, as given in Table IV, it can be observed that among eight methods, MSDivEn-SVM method obtains the highest classification accuracy with the smallest standard deviation. It confirms the advantage of MSDivEn in feature extraction. For the time consumption comparison, it can be seen that MSDivEn has the highest calculation efficiency among seven methods except SDivEn. It implies that MSDivEn not only performs well in feature extraction, but also meets the online detection requirements for real applications.

To facilitate visualization, t-SNE method is utilized to obtain 2-D visualization figures as illustrated in Fig. 14. Seen from Fig. 14(a), for MSDivEn, it can observed that there is a distinct class center for each class and few samples scatter from the class center, which will make it easy for SVM classifier to classify. For MFE, the class center of classes 2, 4, 7, and 8 is clear, but the class center of classes 1 3, 5, and 8 are ambiguous. On the contrary, each category is scattered and the boundary is indistinguishable for MSE and MPE method. In summary, compare with MPE, MFE, and MSE, there is a nice boundary and distinct class center of each class for MSDivEn method, which further validate the feature extraction ability of MSDivEn.

In order to test the robustness of our proposed method, we continuously add white Gaussian noise into the experimental signals. The SNR varies from 0 to -20 dB with the step of 1 dB. The effect of noise on the diagnosis results is conducted between MSDivEn, MSE, MFE, and MPE methods. The comparison results are shown in Fig. 15. As can be seen from Fig. 15, the testing accuracies of all methods decrease with the decreasing of SNR. For MSE, MFE, and MPE methods, the corresponding classification accuracies start decreasing around -10 dB. For the proposed MSDivEn method, the classification accuracies start decreasing around -15 dB. It can be observed that the MSE method achieves the worst performance with

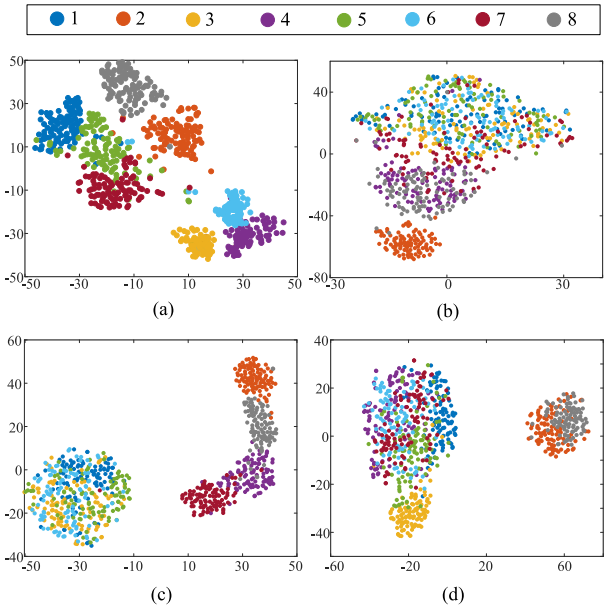

Fig. 14. 2-D feature visualization using t-SNE for four methods. (a) Multiscale symbolic diversity entropy. (b) Multiscale sample entropy. (c) Multiscale fuzzy entropy. (d) Multiscale permutation entropy.

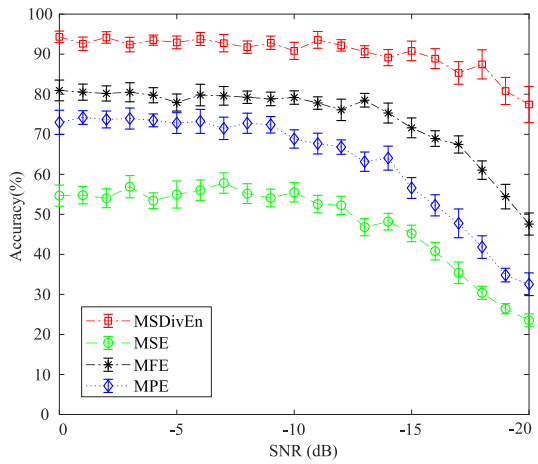

Fig. 15. Testing accuracies of MSDivEn, MSE, MFE, and MPE under different SNR conditions.

the lowest mean testing accuracy among four methods. MPE method benefits from the permutation process, which actually is a kind of symbol dynamic filter, and MFE method benefits from the noise-resistant ability of fuzzy set. Hence, MFE and MPE methods perform better than that of MSE. Moreover, it can be found that the proposed MSDivEn method achieves the highest testing accuracy with smallest decreasing ratio. This indicates the proposed MSDivEn has the best robustness ability to noise, which coincides with the simulated result in Section III-B.

The FFT spectra before and after SDF for the broken tooth on first-stage planet gear are shown in Fig. 16. According to[29], the fundamental meshing frequencies are $f_1 = 168$ Hz for the first gear stage and $f_2 = 182$ Hz for the second gear stage. Note that the fault frequency $f_p = 7.6$ Hz, which is equal to

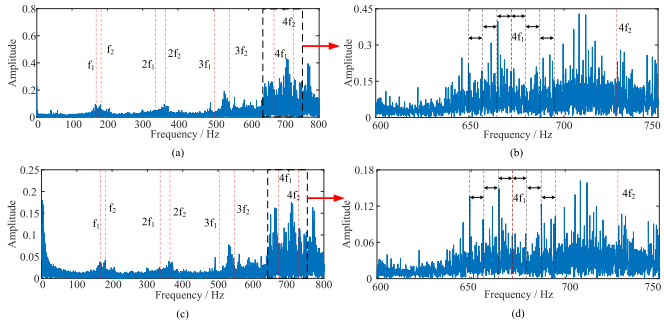

Fig. 16. FFT spectra of the broken tooth on first-stage planet gear. (a) Spectra without SDF. (b) Local amplification spectra without SDF. (c) Spectra with SDF. (d) Local amplification spectra with SDF.

TABLE V
CFIC VALUES OF THESE EIGHT CONDITIONS BEFORE AND AFTER SDF

Condition	1	2	3	4	5	6	7	8
CFIC value without SDF	0.18	0.17	0.16	0.16	0.15	0.17	0.14	0.16
CFIC value after SDF	0.28	0.18	0.27	0.21	0.26	0.24	0.21	0.19

the sideband interval frequency. It can be observed that the sidebands of original signal heavily masked by the background noise without using the SDF. This is because the periodic impacts caused by localized damage have low energy, which is buried in the strong interference noises. By contrast, the fundamental meshing frequencies and sidebands can be clearly observed after SDF-based filtering process. Meanwhile, the FFT spectra after SDF-based filtering process are smoother with fewer burrs.

Moreover, a characteristic frequency intensity coefficient (CFIC) [30] is employed to quantify the performance of the above analysis results, which can be expressed as follows:

$$\mathrm{CFIC} = \sum_{k=1}^{M} A_{kf_c} / \sum_{j=1}^{N} A_{kf_j} \tag{6}$$

where A_{kf_c}represents the amplitude of the kth harmonic of the fault frequency, $A_{kf_j}$is amplitude of the frequency f_j, M is the number of harmonics of the fault frequency, and N is number of frequency components in the frequency spectrum.

The CFIC represents the portion of the fault frequency amplitude to the overall frequency amplitude. Obviously, a larger value of CFIC implies a better fault detection. The CFIC of eight conditions before and after SDF are calculated. In this article, M is set to be 4 and N is set to be 800. The CFIC values of these eight conditions are given in Table V. Seen from Table V, larger CFIC values can be obtained after SDF. The compared results have demonstrated that the proposed method performs best in resisting the noises. It can be concluded that SDF helps to remove the noises and enhance the fault characteristics of planetary gearboxes under the eight conditions in fault detection.

C. Parameter Sensitivity Analysis

The sensitivity analysis of four parameters, including scale parameter τ, dimension m, time lagged variable λ, and the

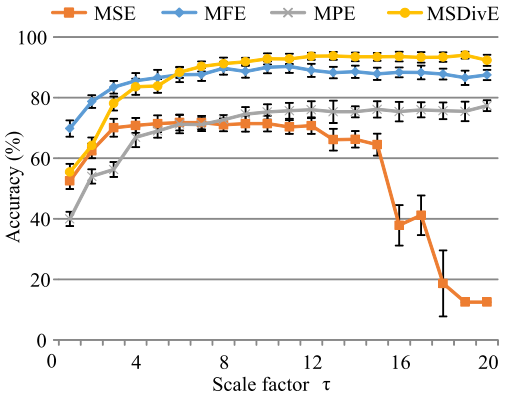

Fig. 17. Diagnosis results using different scale factor τ.

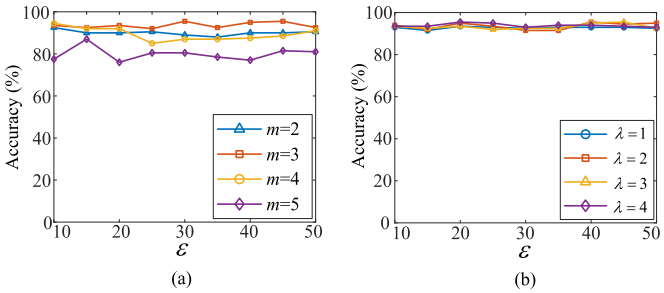

Fig. 18. Parameter sensitivity the dimension m, time lagged variable λ, and the number of symbolsε.

number of symbols ε are considered, and their effects on the final diagnosis performance have been investigated in this article.

To investigate the effect of scale parameter τ on multiscale analysis, the diagnostic performance of MSDivEn with different scale factor τ is tested and the obtained results are shown in Fig. 17. From Fig. 17, it can be observed that, with τ increasing, both the classification accuracy first presents an increasing trend and levels off gradually for MPE, MFE, and MSDivEn method. However, classification accuracy of MSE first increases and then decreases gradually. This is because that the coarse-graining process will reduce the length of a time series considerably at large scales, and SE is thus invalid in analyzing short time series. It is indicated that a too small value of τ will lead to the loss of fault information, while a too large value of τ will lead to information redundancy, which even degrade the classification performance. Therefore, the scale parameter τ is suggested to take 10 to 20.

Next, we will discuss the effect of the dimension m, time lagged variable λ, and the number of symbols ε. The results of MSDivEn under different parameter combinations are illustrated in Fig. 18. From Fig. 18(a), it can be observed that when the ε value is fixed, $m = 3$ obtains the highest classification accuracy. A smaller m obtains less detailed reconstruction information of the dynamic process. Conversely, if the dimension m is too large, it may reduce the numbers of reconstruction vectors, which lead to the loss of some information. Moreover, the valueε also relates to the information reservation of time series. From Fig. 18(a) and (b), it can be found that the classification accuracy seldom changes with the increasing of ε from 10 to 50. This phenomenon indicates that the value ε makes little influence in the range of 10–50. From Fig. 18(b), it can be observed that the time lagged variable λ has limited influence to the final classification accuracy; thus, it thus has little effect on the performance of MSDivEn.

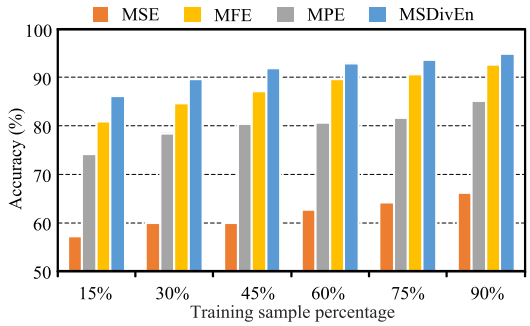

Fig. 19. Effect of training sample size for MSDivEn, MSE, MFE, and MPE methods.

We also tested the performance of our proposed method using different percentages of samples as training samples (the remaining samples will be considered as test samples). Six percentages were tested: 15%, 30%, 45%, 60%, 75%, and 90%. To reduce randomness, 20 trails were conducted for each percentage. The averaging testing accuracies were calculated and illustrated in Fig. 19. It can be observed that the testing accuracy increases with the increase training samples for all entropy methods. However, the proposed MSDivEn method can still obtain the highest classification accuracy with different training sample size among the four methods. The comparison results validate the superiority of MSDivEn method in extracting weak characteristics of planetary gearboxes.

V. Conclusion

In this article, a novel complexity analysis algorithm, namely SDivEn, was proposed to measure the regularity or orderliness of the time series. Compared to other entropy methods, SDF and the concept of distribution are introduced for complexity measurement. Multiple simulated signals were used to verify the merits of SDivEn in consistency, robustness to noises, and high calculation efficiency. Aside from that, to increase the feature representation capability of entropy descriptors, multiscale analysis was performed, namely MSDivEn, which was applied for condition recognizing of planetary gearboxes. The proposed method achieves the highest average classification accuracy of 93.42% in recognizing seven fault types of a planetary gearbox compared with MSE, MFE, and MPE methods. Moreover, we proves that MSDivEn performs better than MPE, MFE, and MSE methods in two categories: MSDivEn does a better job in removing environment noises while preserving information; and it has a higher calculation efficiency. This implies that the proposed method was used for online health condition monitoring and diagnosis.

In this article, the proposed MSDivEn method was tested and demonstrated to be effective in diagnosing several faults of constant load torque and speed. However, the effectiveness of variable speed/variable load torque was unknown. In our future work, we will test the effectiveness of MSDivEn in the variable working conditions combined with order-tracking technique, such as Vold–Kalman filter. Moreover, the fault mechanism based entropy fault diagnosis method will be further studied through dynamic equations and responses.

REFERENCES

[1] L. Wang, Z. Zhang, H. Long, J. Xu, and R. Liu, "Wind turbine gearbox failure identification with deep neural networks," *IEEE Trans. Ind. Informat.*, vol. 13, no. 3, pp. 1360–1368, Jun. 2017.

[2] Z. Feng and M. J. Zuo, "Vibration signal models for fault diagnosis of planetary gearboxes," *J. Sound Vib.*, vol. 331, no. 22, pp. 4919–4939, Oct. 2012.

[3] M. Zhang, K. Wang, D. Wei, and M. J. Zuo, "Amplitudes of characteristic frequencies for fault diagnosis of planetary gearbox," *J. Sound Vib.*, vol. 432, pp. 119–132, Oct. 2018.

[4] K. Zhang, B. Tang, Y. Qin, and L. Deng, "Fault diagnosis of planetary gearbox using a novel semi-supervised method of multiple association layers networks," *Mech. Syst. Signal Process.*, vol. 131, pp. 243–260, Sep. 2019.

[5] S. R. Saufi, Z. A. Bin Ahmad, M. S. Leong, and M. H. Lim, "Gearbox fault diagnosis using a deep learning model with limited data sample," *IEEE Trans. Ind. Informat.*, vol. 16, no. 10, pp. 6263–6271, Oct. 2020.

[6] J. Yu and X. Zhou, "One-Dimensional residual convolutional autoencoder based feature learning for gearbox fault diagnosis," *IEEE Trans. Ind. Informat.*, vol. 16, no. 10, pp. 6347–6358, Oct. 2020.

[7] Y. Li, Y. Yang, X. Wang, B. Liu, and X. Liang, "Early fault diagnosis of rolling bearings based on hierarchical symbol dynamic entropy and binary tree support vector machine," *J. Sound Vib.*, vol. 428, pp. 72–86, 2018.

[8] Y. Li, K. Feng, X. Liang, and M. J. Zuo, "A fault diagnosis method for planetary gearboxes under non-stationary working conditions using improved Vold–Kalman filter and multi-scale sample entropy," *J. Sound Vib.*, vol. 439, pp. 271–286, Jan. 2019.

[9] J. Zheng, H. Pan, and J. Cheng, "Rolling bearing fault detection and diagnosis based on composite multiscale fuzzy entropy and ensemble support vector machines," *Mech. Syst. Signal Process.*, vol. 85, pp. 746–759, Feb. 2017.

[10] C. Bandt and B. Pompe, "Permutation entropy: A natural complexity measure for time series," *Phys. Rev. Lett.*, vol. 88, no. 17, Apr. 2002, Art. no. 174102.

[11] X. Zhang, Y. Liang, J. Zhou, and Y. Zang, "A novel bearing fault diagnosis model integrated permutation entropy, ensemble empirical mode decomposition and optimized SVM," *Measurement*, vol. 69, pp. 164–179, Jun. 2015.

[12] G. Cheng, X. Chen, H. Li, P. Li, and H. Liu, "Study on planetary gear fault diagnosis based on entropy feature fusion of ensemble empirical mode decomposition," *Measurement*, vol. 91, pp. 140–154, Sep. 2016.

[13] Y. Li, G. Li, Y. Yang, X. Liang, and M. Xu, "A fault diagnosis scheme for planetary gearboxes using adaptive multi-scale morphology filter and modified hierarchical permutation entropy," *Mech. Syst. Signal Process.*, vol. 105, pp. 319–337, May 2018.

[14] S. D. Wu, C. W. Wu, S. G. Lin, K. Y. Lee, and C. K. Peng, "Analysis of complex time series using refined composite multiscale entropy," *Phys. Lett. A*, vol. 378, no. 20, pp. 1369–1374, 2014.

[15] T.-Y. Wu, C.-L. Yu, and D.-C. Liu, "On multi-scale entropy analysis of order-tracking measurement for bearing fault diagnosis under variable speed," *Entropy*, vol. 18, no. 8, Aug. 2016, Art. no. 292.

[16] Y. Li, X. Wang, S. Si, and S. Huang, "Entropy based fault classification using the case western reserve university data: A benchmark study," *IEEE Trans. Rel.*, vol. 69, no. 2, pp. 754–767, Jun. 2020..

[17] V. Rajagopalan and A. Ray, "Symbolic time series analysis via wavelet-based partitioning," *Signal Process*, vol. 86, no. 11, pp. 3309–3320, Nov. 2006.

[18] A. Ray, "Symbolic dynamic analysis of complex systems for anomaly detection," *Signal Process*, vol. 84, no. 7, pp. 1115–1130, Jul. 2004.

[19] P. B. Graben, "Estimating and improving the signal-to-noise ratio of time series by symbolic dynamics," *Phys. Rev. E*, vol. 64, no. 5, Oct. 2001, Art. no. 051104.

[20] J. Yu, J. Cao, W.-H. Liao, Y. Chen, J. Lin, and R. Liu, "Multivariate multiscale symbolic entropy analysis of human gait signals," *Entropy*, vol. 19, no. 10, Oct. 2017, Art. no. 557.

[21] M. Srivastava, C. L. Anderson, and J. H. Freed, "A new wavelet denoising method for selecting decomposition levels and noise thresholds," *IEEE Access*, vol. 4, pp. 3862–3877, 2016.

[22] W. Chen, Z. Wang, H. Xie, and W. Yu, "Characterization of surface EMG signal based on fuzzy entropy," *IEEE Trans. Neural Syst. Rehabil. Eng.*, vol. 15, no. 2, pp. 266–272, Jun. 2007.

[23] X. Liang, M. J. Zuo, and M. R. Hoseini, "Vibration signal modeling of a planetary gear set for tooth crack detection," *Eng. Failure Anal.*, vol. 48, pp. 185–200, Feb. 2015.

[24] J. Zheng, J. Cheng, and Y. Yang, "Multiscale permutation entropy based rolling bearing fault diagnosis," *Shock Vib.*, vol. 2014, Mar. 2014, Paper e154291.

[25] S. M. Pincus, "Approximate entropy as a measure of system complexity," *Proc. Nat. Acad. Sci.*, vol. 88, no. 6, pp. 2297–2301, Mar. 1991.

[26] R. Yan and R. X. Gao, "Approximate entropy as a diagnostic tool for machine health monitoring," *Mech. Syst. Signal Process.*, vol. 21, no. 2, pp. 824–839, Feb. 2007.

[27] G. Li, F. Li, Y. Wang, and D. Dong, "Fault diagnosis for a multistage planetary gear set using model-based simulation and experimental investigation," *Shock Vib.*, vol. 2016, 2016, Art. no. 9263298.

[28] H.-L. Chen, B. Yang, J. Liu, and D.-Y. Liu, "A support vector machine classifier with rough set-based feature selection for breast cancer diagnosis," *Expert Syst. Appl.*, vol. 38, no. 7, pp. 9014–9022, Jul. 2011.

[29] G. Li, F. Li, H. Liu, and D. Dong, "Fault features analysis of a compound planetary gear set with damaged planet gears," *Proc. Inst. Mech. Eng. Part C J. Mech. Eng. Sci.*, vol. 232, no. 9, pp. 1586–1604, May 2018.

[30] B. Li, P. Zhang, Z. Wang, S. Mi, and Y. Zhang, "Gear fault detection using multi-scale morphological filters," *Measurement*, vol. 44, no. 10, pp. 2078–2089, Dec. 2011.